Defence Technology 14 (2018) 709–719

Contents lists available at ScienceDirect

Defence Technology

journal homepage: www.elsevier.com/locate/dt

Influence of control strategy on stability of dual-spin projectiles with fixed canards

Yu Wang*, Xiao-ming Wang, Ji-yan Yu

Nanjing University of Science & Technology, School of Mechanical Engineering, 210094, Nanjing, People's Republic of China

ARTICLE INFO

Article history:
Received 16 December 2017
Received in revised form
22 February 2018
Accepted 17 April 2018
Available online 4 May 2018

Keywords:
Dual-spin projectile
Fixed canards
Control strategy
Flight stability

ABSTRACT

Existing literature has shown that the control force at the nose could cause dynamic instability for controlled projectiles. To lower the adverse impact on the dual-spin projectile with fixed canards under the premise of meeting guidance system requirements, the influence of control moment provided by a motor on the flight stability is analyzed in this paper. Firstly, the effect of the rolling movement on stability is analyzed based on the stability criterion derived using the Hurwitz stability theory. Secondly, the evaluation parameters combining the features of different control periods that could assess the variation of stability features after the motor torque are obtained. These effective formulas are used to indicate that, to reduce the flight instability risks, the stabilized rolling speed of roll speed keeping period should be as small as possible; the variation trend of motor torque during the rolling speed controlling period and the roll angle of the forward body during roll angle switching period are recommended corresponding to the projectile and trajectory characteristics. Moreover, detailed numerical simulations of 155 mm dual-spin projectile are satisfactory agreement with the theoretical results.

1. Introduction

Undoubtedly, low collateral damage and high strike precision are the increasing requirements of the modern and future battlefield. To this purpose, interest in retrofitting the large stockpile of existing conventional munitions to possess trajectory correction capability has led to the development of several programs [1–6] over the past four decades. Because the extremely high spin rates of the spin-stabilized projectile will bring severe technical challenges for smart-weapon designers, the concept of roll-decoupled course correction fuse with canards was proposed.

Costello et al. [7] developed a dual-spin projectile seven degree-of-freedom (7DOF) dynamic model and discussed the dynamic and the gyroscopic stability by using projectile linear theory applicable for this projectile without canards. Wernert [8] studied the stability of canard-guided dual-spin projectile by virtue of a linearized model of the pitching and yawing motion. Zhu et al. [9] deduced a stability criterion for such a projectile utilizing the linear theory, Murphy's complex variable method and Hurwitz stability theory. Ollerenshaw [10] and Fresconi [11] analyzed the swerve response of spin-stabilized projectiles to control mechanism inputs, and demonstrated that the phase shift of the swerve response is close to 180° when the control mechanism is located near the nose of projectile. Chang [12] explored the dynamic response to control input by considering the coupled effect of canard control and gravity, and indicated that the phase shift may vary substantially with different deflection angles of canards during the process of guidance and control. Theodoulis et al. [13] analyzed the airframe stability for operating points of the flight envelop in terms of the quasi-linear parameter-varying model and presented a complete design concerning the guidance and autopilot modules for a class of spin-stabilized fin-controlled projectiles. Frank Fresconi [14] derived a guidance and control strategy based on flight dynamics that enables precision and trajectory shaping with reduced sensor and actuator needs.

The work here aims at the dual-spin projectile with two sets of fixed canards [15] (shown in Fig. 1): a pair of spin canards (canards 1–3) and a pair of steering canards (canards 2–4). In a bank-to-turn approach, steering is accomplished by stabilizing the forward body at the appropriate roll angle to create lift in a desired direction with the motor. Contrary to the extensive literature on

* Corresponding author.
E-mail address: 15250996016@163.com (Y. Wang).
Peer review under responsibility of China Ordnance Society

https://doi.org/10.1016/j.dt.2018.04.014

Nomenclature

C_D	drag force coefficient for the whole projectile;
$C_{L\alpha}$	lift force coefficient for the whole projectile;
$C^A_{Mp\alpha}, C^F_{Mp\alpha}$	Magnus moment coefficient for the aft and forward bodies
C_{Mq}	damping moment coefficient for the whole projectile;
$C_{M\alpha}$	static moment coefficient for the whole projectile;
$C_{M\dot{\alpha}}$	pitch damping moment coefficient due to the change rate of the angle of attack
$C_{N\delta}$	normal control force coefficient for steering canards
C_{rc}	roll moment aerodynamic coefficient due to for the spin canards
C_{rdF},C_{rdA}	roll damping moment aerodynamic coefficient for the forward and aft bodies
c_R	rolling friction coefficient for bearing
c_V	viscous damping coefficient for bearing
F_c	normal control force due to the steering canards
g	gravity acceleration
I_{xA}, I_{xF}	axial moment of inertia of the aft and forward parts
I_y	transverse moment of inertia of the whole projectile;
$I_n()$	the n-ple time integral of ()
i	imaginary unit
l	reference length
l_{CG}	distance between the point of mass and the acting point of the control force due to canards
M_c	control moment due to steering canards
M_{mo}	motor torque
M_{moS}	the balancing motor torque of the forward body
M_{rb}	remaining rolling moment come from the bearing
M_{rc}	roll moment due to spin canards
M_{rdA},M_{rdF}	roll damping moment acting on the aft and forward bodies
M_{xA}, M_{yA}, M_{zA}	total external moment components on the aft body expressed in the fixed-plane frame
M_{xF}, M_{yF}, M_{zF}	total external moment components on the forward body expressed in the fixed-plane frame
m, m_A, m_F	the mass of the total projectile, aft and forward body
p_A, p_F	the rolling speed of the aft and forward body
q, r	pitch and yaw rates expressed in the fixed-plane frame
S	reference area
u, v, w	projectile velocity components expressed in the fixed-plane frame
V	velocity magnitude of projectile composite mass center
X_A, Y_A, Z_A	total external force components on the aft body expressed in the fixed-plane frame
X_F, Y_F, Z_F	total external force components on the forward body expressed in the fixed-plane frame
α, β	angle of attack and sideslip in the fixed-plane frame
α_e, β_e	trim angles of attack and sideslip;
δ_s	deflect angle of steering canards
ΔM_{mo}	the difference between the actual and balancing motor torque of the forward body
ξ	$\beta + i\alpha$
γ_A, γ_F	roll angle of the aft and forward body
ρ	air density
θ	Euler pitch angle
θ_e	steady Euler pitch angle
$()^*$	$()\cdot\rho Sl/(2m)$except for g^*

several aspects regarding this projectile, such as general design, aerodynamics [16], dynamic response, flight stability and guidance, research on the influence of control strategy on the stability of the dual-spin projectile with fixed canards is, to the authors' knowledge, very limited.

This paper investigates the affecting laws of control moment on flight stability of a dual-spin projectile, which can provide a foundation for structure and controlling plan design. The article begins with a description of the differential equation for the complex angle of attack utilizing the projectile linear theory and Murphy's complex variable method. Then the stability criterion and the influence of control moment on flight stability in different control periods are derived. Finally, numerical simulation results and concluding remarks are provided.

2. Stability analysis

For the sake of simplicity, a simplified 7DOF dynamic model whose general case was studied by Costello [7] is established based on the assumption that.

(1) The projectile is nearly aerodynamic symmetric and mass balanced;
(2) The composite center of mass locates on the longitudinal symmetry axis;
(3) Only the roll constrain moment is considered between the forward and the aft bodies;

The translational and rotational dynamic equations of motion are expressed in the fixed-plane frame as

$$\begin{cases} \dot{u} + qw - rv = \dfrac{X_F + X_A}{m} \\ \dot{v} + ru - w\dot{\varphi}_{FP} = \dfrac{Y_F + Y_A}{m} \\ \dot{w} - qu + v\dot{\varphi}_{FP} = \dfrac{Z_F + Z_A}{m} \end{cases} \tag{1}$$

$$\begin{cases} I_{xF}\dot{p}_F = M_{xF} \\ I_{xA}\dot{p}_A = M_{xA} \\ I_y\dot{q} + \left(I^A_x p_A + I^F_x p_F\right)r + I_y r\dot{\varphi}_{FP} = M_{yF} + M_{yA} \\ I_y\dot{r} - (I_{xA}p_A + I_{xF}p_F)q - I_y q\dot{\varphi}_{FP} = M_{zF} + M_{zA} \end{cases}$$

Where $\dot{\varphi}_{FP} = -r\tan\theta$.

The dynamic model of the dual-spin projectile with fixed canards is almost the same with that with cruciform canards other than the control force, control moment and the motor moment acting on the axis-direction. Referring to the model in Refs. [9] and [12], the control force and control moment of a dual-spin projectile due to fixed canards in the fixed-plane reference frame can be calculated by

$$F_C \approx \frac{\rho S V^2}{2} C_{N\delta}\left(\delta_s \begin{bmatrix} 0 \\ \cos\gamma_F \\ \sin\gamma_F \end{bmatrix} + \begin{bmatrix} 0 \\ \alpha \\ \beta \end{bmatrix}\right)\mathbb{k} \tag{2}$$

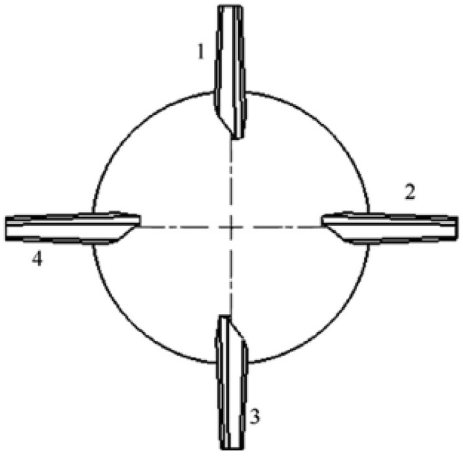

Fig. 1. Diagram of canards.

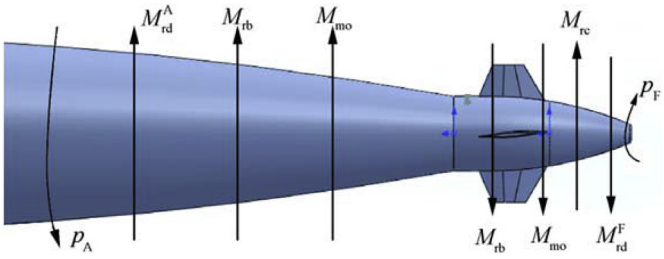

Fig. 2. The rolling moments acting on the forward and aft bodies.

$$M_C \approx \frac{\rho S V^2 l_{CG}}{2} C_{N\delta} \left(\delta_s \begin{bmatrix} 0 \\ -\sin\gamma_F \\ \cos\gamma_F \end{bmatrix} + \begin{bmatrix} 0 \\ -\beta \\ \alpha \end{bmatrix} \right) \tag{3}$$

The structure schematic of the dual-spin projectile and the moments on the longitudinal symmetry axis of the projectile are shown in Fig. 2. The rolling moments come from the bearing M_{rb} and motor M_{mo} are acting on the forward and aft body in the opposite direction. The roll damping moments M_{rdA} and M_{rdF} which can be calculated by equation (4) are acting on the aft and forward body respectively. C_{rdF} here is a negative number; C_{rdA} here is a positive number. In order to ensure the normal operation of the correction course fuse, a negative roll moment due to the spin canards (shown in equation (5)) is acting on the forward body.

$$\begin{cases} M_{rd}^{F} = 0.5\rho S l^2 V p_F C_{rdF} \\ M_{rd}^{A} = 0.5\rho S l^2 V p_A C_{rdA} \end{cases} \tag{4}$$

$$M_{rc} = 0.5\rho V^2 S l C_{rc} \tag{5}$$

Substituting these moments into the dynamic equation (1), the rolling dynamic equations of the forward and aft parts are expressed in the fixed-plane frame

$$\begin{cases} I_x^F \dot{p}_F = M_{xF} = M_{rb} - M_{rc} + M_{mo} + M_{rdF} \\ I_x^A \dot{p}_A = M_{xA} = -M_{mo} - M_{rb} - M_{rdA} \end{cases} \tag{6}$$

Corresponding to directions of these moments shown in Fig. 2 and the dynamic equations shown as equation (6), C_{rdF} is negative, and C_{rc}, C_{rdA} are positive.

The remaining rolling moment come from bearing M_{rb} is composed of the viscous damping and rolling friction. The moments acting on the axis-direction of projectile can be written as [7].

$$M_{rb} = c_V(p_A - p_F) + c_R|F_N|sign(p_A - p_F) \tag{7}$$

where the absolute value of normal force acting on the bearing $|F_N|$ is related to the axial force of the forward and aft part.

By using Murphy's method [17] and the linear theory for projectile, the differential equation of complex angle of attack can be written as

$$\xi'' + (H - 2g^* - iP)\xi' - (M + iPT)\xi = \widehat{G} + C + \Phi \tag{8}$$

Where

$\xi = \beta + i\alpha; k_t^{-2} = \sqrt{I_y(ml^2)^{-1}}; H = C_{L\alpha}^* - C_D^* - k_t^{-2}(C_{Mq}^* + C_{M\dot{\alpha}}^*);$
$P = l(I_{xF}p_F + I_{xA} \quad p_A)(I_y V)^{-1}; \quad g^* = gl\sin\theta V^{-2}; M = k_t^{-2}(C_{Nd}^* l_{CG} l^{-1}$
$+C_{M\alpha}^*); T = C_{L\alpha}^* - g^* + lk_t^{-2}P^{-1}V^{-1}(C_{Mp\alpha F}^* p_F + C_{Mp\alpha A}^* p_A); \Phi = -i[\varphi_{FP}''$
$+(H - 2g^* - iP + k_t^{-2}C_{M\dot{\alpha}}^*)\varphi_{FP}']\xi + \varphi_{FP}'^2\xi - i\varphi_{FP}'(2\xi' - igl\cos\theta V^{-2});$
$\widehat{G} = -i(C_D^* + g^* + k_t^{-2}C_{Mq}^* + iP)gl\cos\theta V^{-2}; C = -k_t^{-2}C_{N\delta}^*\delta_s e^{i\gamma_F} l_{CG}/l.$

Linearized at the equilibrium point of equation (8), Φ could be estimated as $-i\xi_e \tan\theta_e[\beta'' + (H - 2g^* - iP)\beta']$, so the equation of complex angle of attack can be rewritten as

$$\begin{aligned} &(1 + \varepsilon\xi_e i)\left[\xi'' + (H - 2g^* - iP)\xi'\right] - (M + iPT)(\xi - \xi_e) \\ &= -\varepsilon\xi_e i\left[\overline{\xi}'' + (H - 2g^* - iP)\overline{\xi}'\right] \end{aligned} \tag{9}$$

Where $\overline{\xi} = \beta - i\alpha; \varepsilon = 0.5\tan\theta_e$. By the coefficient freezing way, the equilibrium point of equation (8) can be expressed as

$$\xi_e = -\frac{\widehat{G} + C}{M + iPT} = \beta_e + i\alpha_e$$

$$\begin{cases} \beta_e = \dfrac{k_t^{-2}C_{Nd}^*\delta_s l_{CG}\cos\gamma_F l^{-1} - gPl\cos\theta V^{-2}}{M^2 + P^2T^2} \\ \alpha_e = \dfrac{\left(C_D^* + g^* + k_t^{-2}C_{Mq}^*\right)gl\cos\theta V^{-2} + k_t^{-2}C_{Nd}^* l_{CG}\delta_s\sin\gamma_F l^{-1}}{M^2 + P^2T^2} \end{cases} \tag{10}$$

By comparison with the complex angle of attack of a dual-spin projectile with cruciform canards deduced in Ref. [9], equation (9) has a good consistency with that of cruciform canards on the form and difference on the parameters, such as M and C. Hence, according to the Hurwitz stability criterion, the stability criteria for the projectile with fixed canards shown in inequalities(11) are similar to those derived in Ref. [9].

$$\begin{cases} p_1 = 2(H - 2g^*) > 0 \\ p_2 > 0 \\ C_{dyna} = \tilde{S}_d\left(2 - \tilde{S}_d\right) - \tilde{S}_g^{-1} > 0 \end{cases} \tag{11}$$

Where $p_2 = (H - 2g^*)^2 + P^2 - (2 - 2\varepsilon\alpha_e)M/(1 - 2\varepsilon\alpha_e) - 2\varepsilon\beta_e PT/(1 - 2\varepsilon\alpha_e); \tilde{S}_d = 2T/\tilde{H}; \tilde{M} \approx M/(1 - \varepsilon\alpha_e) + \varepsilon\beta_e PT/(1 - \varepsilon\alpha_e)^2 + \varepsilon\beta_e PM/[(1 - \varepsilon\alpha_e)\tilde{H}]; \tilde{H} = (1 - \varepsilon\alpha_e)(H - 2g^*); \tilde{S}_g = P^2/(4\tilde{M}).$

3. Control strategy influence on stability

Since the wingspan and deflection angle of canards are immutable, the rolling speed and roll angle of the forward body of this projectile are controlled by the motor torque exactly. Therefore, the control strategy of the dual-spin projectile with fixed canards means the motor torque during the control period in order to satisfy the requirements of guidance system. Neglecting the indirect effect of the motor torque on the Magnus force and Magnus moment, the changing of the motor torque only affects the rolling movement, which includes the rolling speed and roll angle of the forward and aft bodies $p_A, p_F, \gamma_A, \gamma_F$.

For the sake of simplicity, the study on the influence on stability of control strategy is divided into two steps: the analysis on the effects of the rolling movement on stability and the control strategy on rolling movement. The main problem in the first step is the influence law of the rolling movement on the stability parameters. The second step is to study the dependences of the rolling movement parameters corresponding to the results obtained in the first step on the control strategy.

3.1. Impact of rolling movement on stability

As is known to all, the stability margin indicates the distance between the operating point and the critical stable state. The influence of the control strategy on the stability is transformed into an optimization of the stability margin under different control strategies. Because of stability of this projectile is assessed through three parameters p_1, p_2 and C_{dyna} synchronously, the influence on stability should take these three aspects into account comprehensively.

3.1.1. The first stability parameter p_1

According to the aforementioned analysis, it is reasonable to assume that with the variation of control strategy-the motor torque, only the rolling movement- $p_A, p_F, \gamma_A, \gamma_F$ varies, other than the other trajectory characteristics such as velocity, the pitch angle et al. Therefore, the parameters unrelated to rolling movement such as g^*, H, M, k_t^{-2}, are independent from the control strategy. Considering the definition $p_1 = 2(H - 2g^*)$, the first stability parameter p_1 is invariant with the rolling movement as well as the control strategy.

3.1.2. The second stability parameter p_2

In view of the definition of p_2, the variation of this stability parameter under different $p_A, p_F, \gamma_A, \gamma_F$ can be expressed as

$$\Delta p_2 = \Delta P^2 - M\Delta\left(\frac{2-2\varepsilon\alpha_e}{1-2\varepsilon\alpha_e}\right) - \Delta\left(\frac{2\varepsilon\beta_e}{1-2\varepsilon\alpha_e}PT\right) \tag{12}$$

Since $|PT|$ is usually much smaller than M [18], neglecting the variation of β_e under different rolling movement and letting $1-2\varepsilon\alpha_e \approx 1$ and $1-\varepsilon\alpha_e \approx 1$, equation (12) can be calculated approximately as

$$\Delta p_2 \approx \Delta P^2 - \tan\theta_e\beta_e\Delta(PT) \tag{13}$$

To simplify the analysis, the rolling speeds corresponding to this stability characteristic p_2 to be compared are recorded as $p_A + \Delta p_A$, $p_F + \Delta p_F$ and p_A, p_F respectively. As the moment of inertial is the inherent property of the projectile, and the variation of velocity caused by different control strategies is small enough to be neglected, Δp_2 is a function that depends on p_A, p_F, Δp_F and Δp_A. Compared with p_A -dependent term, it is reasonable to neglect the terms correlated to p_F, Δp_F, Δp_A and the starred coefficients along with trim angle of sideslip β_e, so that Δp_2 shown in equation can be simplified and rewritten as

$$\Delta p_2 \approx \frac{2I^2 I_{xA} p_A}{I_y^2 V^2}\left(I_{xF}\Delta p_F + I_{xA}\Delta p_A\right) \tag{14}$$

According to the stability criterion $p_2 > 0$ and equation (14), the stability corresponding to p_2 will ascend with the increasing of Δp_2, in other words, the stability corresponding to p_2 will increase when $I_{xF}\Delta p_F + I_{xA}\Delta p_A > 0$; otherwise, the stability will weaken.

3.1.3. The third stability parameter C_{dyna}

According to dynamic stability condition shown as the third inequality of criterion(11), the dynamic stability is enhanced with increasing of C_{dyna}. Similarly to the analysis in the previous section, the rolling speeds corresponding to the dynamic criterion characteristic C_{dyna} to be compared are recorded as $p_A + \Delta p_A$, $p_F + \Delta p_F$ and p_A, p_F respectively. Substituting the aforementioned definition of $\tilde{S}_d$ and $\tilde{S}_g$, the variation of C_{dyna} under different rolling speeds of the forward and aft bodies can be expressed as

$$\begin{aligned}\Delta C_{dyna} &= \Delta\left(\tilde{S}_d\left(2-\tilde{S}_d\right) - 1\Big/\tilde{S}_g\right)\\ &= \Delta\left(A + (2-A)\varphi - \varphi^2 - \lambda\right)\\ &= (2-A)\Delta\varphi - \Delta\varphi^2 - \Delta\lambda\end{aligned} \tag{15}$$

Where $\varphi = I_y k_t^{-2}(C^*_{Mp\alpha F}p_F + C^*_{Mp\alpha A}p_A)/[\tilde{H}(I_{xF}p_F + I_{xA}p_A)]$, $\lambda = 4\tilde{M}I_y^2V^2/[I^2(I_{xF}p_F + I_{xA}p_A)^2]$, $A = (2C^*_{L\alpha} - g^*)/\tilde{H}$.

As the rolling speed of the aft body are much larger than that of the forward body and variations of these rolling speed caused by control, $\Delta\lambda$, $\Delta\Phi$ and $\Delta\Phi^2$ can be calculated and simplified as

$$\Delta\lambda = \frac{4\tilde{M}I_y^2V^2}{I^2}\frac{(I_{xF}p_F + I_{xA}p_A)^2 - [I_{xF}(p_F+\Delta p_F) + I_{xA}(p_A+\Delta p_A)]^2}{(I_{xF}p_F + I_{xA}p_A)^2[I_{xF}(p_F+\Delta p_F) + I_{xA}(p_A+\Delta p_A)]^2} \tag{16}$$

Substituting equations (16) and (17)into equation (15), the dynamic criterion characteristic neglecting the small values can be rewritten as

$$\begin{aligned}\Delta\Phi &= \frac{I_y k_t^{-2}}{\tilde{H}}\left(\frac{C^*_{Mp\alpha F}(p_F+\Delta p_F) + C^*_{Mp\alpha A}(p_A+\Delta p_A)}{I_{xF}(p_F+\Delta p_F) + I_{xA}(p_A+\Delta p_A)} - \frac{C^*_{Mp\alpha F}p_F + C^*_{Mp\alpha A}p_A}{I_{xF}p_F + I_{xA}p_A}\right)\\ &\approx -\frac{I_y k_t^{-2}}{\tilde{H}}\frac{\Delta p_F\left(I_{xF}C^{A*}_{Mp\alpha} - I_{xA}C^{F*}_{Mp\alpha}\right)}{I_{xA}^2(p_A+\Delta p_A)}\end{aligned} \tag{17}$$

$$\begin{aligned}\Delta\Phi^2 &= \left(\frac{I_y k_t^{-2}}{\tilde{H}}\right)^2\left[\left(\frac{C^*_{Mp\alpha F}(p_F+\Delta p_F)+C^*_{Mp\alpha A}(p_A+\Delta p_A)}{I^F_x(p_F+\Delta p_F)+I^A_x(p_A+\Delta p_A)}\right)^2-\left(\frac{C^*_{Mp\alpha F}p_F+C^*_{Mp\alpha A}p_A}{I^F_x p_F+I^A_x p_A}\right)^2\right]\\ &\approx -\left(\frac{I_y k_t^{-2}}{\tilde{H}}\right)^2\frac{\Delta p_F\left(I_{xF}C^*_{Mp\alpha A}-I_{xA}C^*_{Mp\alpha F}\right)\left[C^*_{Mp\alpha F}(2p_F+\Delta p_F)+C^*_{Mp\alpha A}(2p_A+\Delta p_A)\right]}{I^3_{xA}p^2_A}\end{aligned} \tag{18}$$

$$\Delta C_{dyna}=(K_1+K_2I_{xF})\Delta p_F+K_2I_{xA}\Delta p_A$$

$$\begin{cases}K_1=\dfrac{I_y k_t^{-2}\left(I_{xF}C^*_{Mp\alpha A}-I_{xA}C^*_{Mp\alpha F}\right)}{\tilde{H}I^2_{xA}p_A}\left(\dfrac{2I_y k_t^{-2}C^*_{Mp\alpha A}}{\tilde{H}I_{xA}}-(2-A)\right)\\ K_2=\dfrac{8\tilde{M}I^2_y V^2}{l^2(I_{xA}p_A)^3}\end{cases} \tag{19}$$

3.2. Influence of control strategy on stability

According to the aforementioned analyses of the influence of control strategy on the flight stability, the variation of the flight stability is characterized by

$$\begin{cases}\Delta C_{p2}=\dfrac{2l^2I_{xA}p_A}{I^2_y V^2}(I_{xF}\Delta p_F+I_{xA}\Delta p_A)\\ \Delta C_{dyna}=(K_1+K_2I_{xF})\Delta p_F+K_2I_{xA}\Delta p_A\end{cases} \tag{20}$$

where ΔC_{p2} represents the influence on the stability corresponding to the second criterion; ΔC_{dyna} represents the influence on that corresponding to the third one.

As is known to all, the stability margin indicates the distance between the operating point and the critical stable state. It can be seen from equations (14) and (19) that the change of stability margin corresponding to p_2 equals to ΔC_{p2}, and the change of dynamic stability margin equals to ΔC_{dyna}. So the larger these characteristics are, the more stable the projectile is.

To assess the influence on stability synthetically, a function (shown in equation (21)) colligates the relative variation of the second and the third criterion of formula is defined. As the parameters in this function are dynamic, it is a function of time under a specific control strategy.

$$\begin{aligned}G(t)&=\frac{\Delta C_{p2}}{p_2}+\frac{\Delta C_{dyna}}{C_{dyna}}\\ &=\left(\frac{2l^2I_{xA}I_{xF}p_A}{I^2_y V^2 p_2}+\frac{K_1+K_2I_{xF}}{C_{dyna}}\right)\Delta p_F+\left(\frac{2l^2I^2_{xA}p_A I_{xF}}{I^2_y V^2 p_2}+\frac{K_2I_{xA}}{C_{dyna}}\right)\Delta p_A\end{aligned} \tag{21}$$

where p_2 and C_{dyna} are the stability parameters corresponding to the free flight ballistics at the time to study.

For sake of simplicity, the motor torque is divided into two parts: the balancing torque moment of the forward body M_{moS} and the rest moment ΔM_{mo} which is related to the control strategy directly.

Substituting $M_{mo}=M_{moS}+\Delta M_{mo}$ into equation (6), it can be obtained that during roll angle keeping period, the variation rate of the rolling speed of the aft body can be calculated by

$$\begin{cases}I_{xF}\dot{p}_F=\Delta M_{mo}\\ I_{xA}\dot{p}_A=-M_{rc}+M_{rdF}-M_{rdA}-\Delta M_{mo}\end{cases} \tag{22}$$

Assuming the same control strategy is implemented which means ΔM_{mo} is the same, the evaluation parameter shown in equation (21) is proportional to Δp_A whose coefficient is usually positive because of the stability of the free flight projectile should be guaranteed. Therefore the flight stability will increase with the increasing of p_A. Although M_{rdA} is proportional to p_A, the major factor of $\dot{p}_A$ is the driving moments instead of the retardation torque M_{rdA}, which

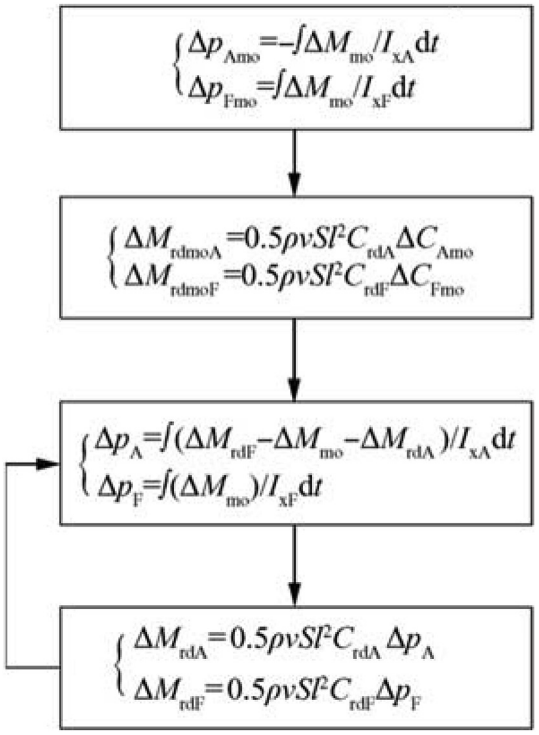

Fig. 3. The calculation flow of $\Delta p_F, \Delta p_A$.

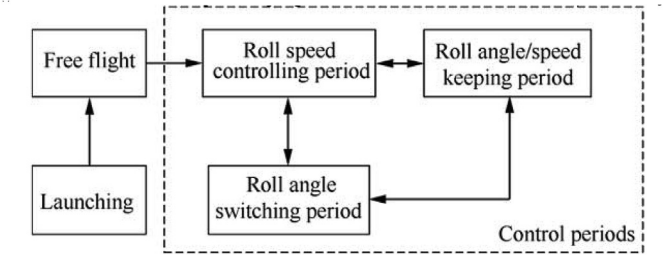

Fig. 4. The flow chart of flight process.

means $\dot{p}_A$ will decrease with increasing M_{rc}. In conclusion, the flight stability of this projectile is strengthening with decreasing M_{rc}, under a determined control strategy. To evade or decrease instability risk of the projectile with fixed canards, a pair of spin canards whose roll moment is as small as possible should be designed.

When the structure of projectile is determined, a variable motor torque characterized by ΔM_{mo} is executed to complete the instructions issued by guidance system. It can be seen from equation (22) that the rolling speed of the aft and forward body are governed by ΔM_{mo}, as well as by the roll damping moments which interact with the rolling speeds. To predigest the calculation of $\Delta p_F, \Delta p_A$ caused by ΔM_{mo}, an iteration method whose derivation process is shown in Fig. 3 is proposed by means of considering the change of rolling speeds as a gradual process. According to the iteration flow shown in Fig. 3, $\Delta p_F, \Delta p_A$ can be expressed as
where $I_n(*)$ represents the n-ple time integral of *. Due to the roll angle variation is the time integral of the corresponding rolling speed variation, $\Delta\gamma_F, \Delta\gamma_A$ can be expressed as

$$\begin{cases} \Delta p_A = \sum_{n=1}^{\infty}\left(-\dfrac{\rho V S l^2 C_{rdA}}{2}\right)^{n-1} I_{xA}^{-n}\left[\dfrac{\rho V S l^2 C_{rdF} I_{n+1}(\Delta M_{mo})}{2I_{xF}} - I_n(\Delta M_{mo})\right] \\ \Delta p_F = \dfrac{I_1(\Delta M_{mo})}{I_{xF}} \end{cases} \tag{23}$$

$$\begin{cases} \Delta\gamma_A = \sum_{n=1}^{\infty}\left(-C^*_{rdA}\right)^{n-1} I_{xA}^{n}\left[\dfrac{C^*_{rdF} I_{n+2}(\Delta M_{mo})}{I_x^F} - I_{n+1}(\Delta M_{mo})\right] \\ \Delta\gamma_F = \dfrac{I_2(\Delta M_{mo})}{I_{xF}} \end{cases} \tag{24}$$

As the terms $\left|C^*_{rdF}/I_{xF}\right|$ and $\left|C^*_{rdA}/I_{xA}\right|$ are much smaller than 1, the higher-order items of equations 23 and 24 can be neglected

To analyze the impact of control strategy namely ΔM_{mo} on the flight stability, substituting equation (25) into equation (20), the

$$\begin{cases} \Delta p_A \approx -I_{xA}^{-1} I_1(\Delta M_{mo}) + 0.5\rho V S l^2 I_{xA}^{-1}\left(C_{rdA} I_{xA}^{-1} + C_{rdF} I_{xF}^{-1}\right) I_2(\Delta M_{mo}) \\ \Delta p_F = I_{xF}^{-1} I_1(\Delta M_{mo}) \\ \Delta\gamma_A \approx -I_{xA}^{-1} I_2(\Delta M_{mo}) + 0.5\rho V S l^2 I_{xA}^{-1}\left(C_{rdA} I_{xA}^{-1} + C_{rdF} I_{xF}^{-1}\right) I_3(\Delta M_{mo}) \\ \Delta\gamma_F = I_{xF}^{-1} I_2(\Delta M_{mo}) \end{cases} \tag{25}$$

characteristics representing the variation of stability can be rewritten as

$$\begin{cases} \Delta C_{p2} = \dfrac{l^4 I_{xA}\rho S p_A}{I_y^2 V}\left(\dfrac{C_{rdA}}{I_{xA}} + \dfrac{C_{rdF}}{I_{xF}}\right) I_2(\Delta M_{mo}) \\ \Delta C_{dyna} = K_1 I_1(\Delta M_{mo}) I_{xF}^{-1} - \dfrac{K_2 \rho V S l^2}{2}\left(\dfrac{C_{rdA}}{I_{xA}} + \dfrac{C_{rdF}}{I_{xF}}\right) I_2(\Delta M_{mo}) \end{cases} \tag{26}$$

Substituting equations (25) and (26) into equation (21), the criterion for assessing the influence on flight stability of control strategy can be rewritten as

$$\begin{aligned} G(t) &= K_3 I_1(\Delta M_{mo}) + K_4 I_2(\Delta M_{mo}) \\ &= I_{xF}(K_3 \Delta p_F + K_4 \Delta\gamma_F) \end{aligned} \quad \begin{cases} K_3 = \dfrac{K_1}{C_{dyna} I_{xF}} \\ K_4 = \rho S l^2\left(\dfrac{C_{rdA}}{I_{xA}} + \dfrac{C_{rdF}}{I_{xF}}\right)\left(\dfrac{l^2 I_{xA} p_A}{I_y^2 V p_2} - \dfrac{K_2 V}{2C_{dyna}}\right) \end{cases} \tag{27}$$

To avoid inconsistency and the potential possibility of resonance [19] caused by the free rotation of the forward body, it is necessary to hold p_F to a specific value rather than non-control when the uncontrolled instruction is issued. Based on the control characters, the control period is divided into four parts (shown in Fig. 4): the roll speed controlling, the roll speed keeping, the roll angle switching and the roll angle keeping period. In the roll speed controlling period, p_F is controlled from one value to another; analogously, γ_F is switched from one value to anther in the roll angle switching period. In the roll angle/speed period, γ_F or p_F remains as a designated value.

After the projectile passes muzzle, a short period of free flight are take place for the initialization of the missile-borne circuit system. Once a signal has been received to start, the rolling speed of the forward body is controlled from a negative value to zero or a specific value in the roll speed controlling period subsequently. And then an adjustment to the roll speed or angle of the forward body required by the guidance system is made. When the guidance system commands stopping control, the control mode is switched into the roll speed controlling period followed by a roll speed keep period. These control periods can switch to each other during the flight process under the command from guidance system.

3.2.1. Roll speed controlling period

As is commanded by the guidance system, the starting and stopping time and the variation of the forward body's rotation speed of this period are immutable. The difference between the forward body's rotation speeds at the starting and ending point is recorded as Δp_{Fv}, and the control time during this period is t_v.

As the stability characteristic shown as equation (27) is variable with the time, it is one-sided to assess the stability at any moment

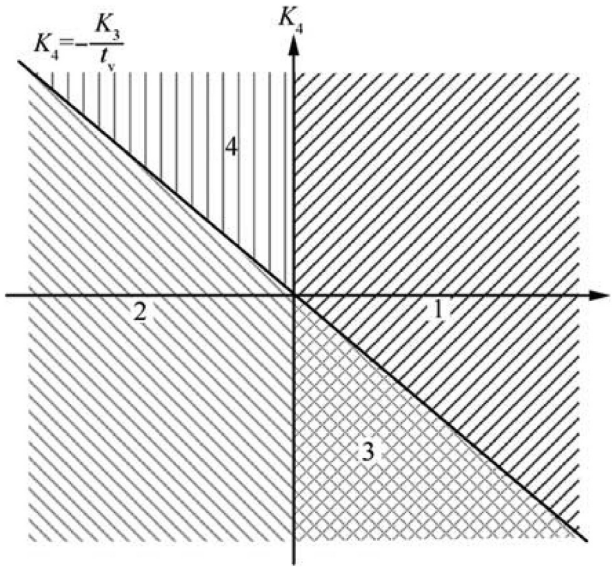

Fig. 5. Zoning map of K_3 and K_4. a) if $K_3>0$ and $K_3+K_4t_v>0$ (zone 1 in Fig. 5), ΔM_{mov} should be monotonically decreasing; b) if $K_3<0$ and $K_3+K_4t_v<0$ (zone 2 in Fig. 5), ΔM_{mov} should be monotonically increasing; c) if $K_3>0$ and $K_3+K_4t_v<0$ (zone 3 in Fig. 5), the ΔM_{mov} increasing before the time of K_3/K_4+t_v and decreasing after that is recommend; d) if $K_3<0$ and $K_3+K_4t_v>0$ (zone 4 in Fig. 5), the ΔM_{mov} decreasing before the time of K_3/K_4+t_v and increasing after that is recommend.

of a period. To assess the stability of this period overall, the stability assessment during a period to be studied should be judged by the integration of $G(t)$, which is recorded as S_p

$$S_p=\int_{t_b}^{t_e}G(t)dt=K_3I_2(\Delta M_{mo})\Big|_{t_b}^{t_e}+K_4I_3(\Delta M_{mo})\Big|_{t_b}^{t_e} \tag{28}$$

Where t_b is the beginning time of the period to be studied, and t_e is the ending time of this period.

For the sake of simplicity, ΔM_{mo} is considered as a superposition of the average and vibration of ΔM_{mo}, which can be recorded as

$$\Delta M_{mo}=\Delta M_{moa}+\Delta M_{mov} \tag{29}$$

Where ΔM_{moa} represents the average of ΔM_{mo}, and ΔM_{mov} represents the vibration during the study period.

Considering the definition of ΔM_{mov} and ΔM_{moa}, the single and double integral of ΔM_{mo} can be expressed as

$$\begin{cases} I_1(\Delta M_{mo})=\Delta M_{moa}t \\ I_2(\Delta M_{mo})=\dfrac{\Delta M_{moa}t^2}{2}+I_2(\Delta M_{mov}) \\ I_3(\Delta M_{mo})=\dfrac{\Delta M_{moa}t^3}{6}+I_3(\Delta M_{mov}) \end{cases} \tag{30}$$

Substituting equation (30) into equation (25) and equation (28), it can be obtained that

$$S_p=\left(\frac{K_3}{2}+\frac{K_4(t_e-t_b)}{6}\right)\Delta p_F I_x^F(t_e-t_b)+K_3I_2(\Delta M_{mov})\Big|_{t_b}^{t_e}+K_4I_3(\Delta M_{mov})\Big|_{t_b}^{t_e} \tag{31}$$

Dividing the control time into n segments, the integrations can be turned into the sums of these segments:

$$\begin{cases} I_2(\Delta M_{mov})\Big|_{t_b}^{t_e}=h^2\sum_{i=1}^{n}(n-i+1)\Delta M_{mov(i)} \\ I_3(\Delta M_{mov})\Big|_{t_b}^{t_e}=h^3\sum_{i=1}^{n}(n-i+1)\dfrac{(n-i+2)}{2}\Delta M_{mov(i)} \end{cases} \tag{32}$$

Where $h=(t_e-t_b)/n=t_v/n$; n is infinity; $\Delta M_{mov(i)}$ is the ΔM_{mov} in the i segment. Hence equation (31) can be rewritten as

$$S_p=\left(\frac{K_3}{2}+\frac{K_4t_v}{6}\right)\Delta p_{Fv}I_{xF}t_v+h^2\sum_{i=1}^{n}\Delta M_{mov(i)}(n-i+1)(K_3+K_4h\frac{(n-i+2)}{2}) \tag{33}$$

As t_v and Δp_{Fv} are invariable, the stability ascends with the increasing of the second item. According to equation (33), S_p has a maximum value when ΔM_{mov} following the change of $(n-i+1)(K_3+K_4h(n-i+2)/2)$. Considering the control time of this period is quite short, K_3 and K_4 may be taken as constants which can be calculated before this period. Consequently, though the analysis of $(n-i+1)(K_3+K_4h(n-i+2)/2)$, the recommend change law of ΔM_{mov} for stability during the roll speed controlling period can be summarized as follows.

Through the deep analysis of the aforementioned preliminary findings, a broad regulation of general application is concluded that ΔM_{mo} should increase when $K_3-K_4(t-t_b-t_v)<0$ and decrease when $K_3-K_4(t-t_b-t_v)>0$ during the roll speed controlling period for the sake of stability.

3.2.2. Roll angle/speed keeping period

During the roll angle or roll speed keeping period, the roll speed of the forward body is held as a designated constant recorded as p_{FK}, which can be described by the equation $\dot{p}_F=0$. Substituting into the first equation of equation (6), it can be obtained that $M_{mo}=M_{moS}=M_{rc}-M_{rb}-M_{rdF}$ and $\Delta M_{mo}=0$ during these periods. In other words, the control strategies of these periods are theoretically definite when p_F is immutable.

Substituting $\Delta M_{mo}=0$ into equation (22), the rotational dynamic equations on the rolling direction can be written as

$$\begin{cases} I_{xA}\dot{p}_A=-M_{rc}+0.5\rho Sl^2V(p_{FK}C_{rdF}-p_AC_{rdA}) \\ \dot{p}_F=0 \end{cases} \tag{34}$$

Because of the roll damping moment of the aft body is the secondary factor in the first equation which cannot change the variation trend of $\dot{p}_A$ and C_{rdF} is negative, $\dot{p}_A$ will decrease with increasing p_{FK} when the roll moment due to spin canards is certain. Combining with the expression of the evaluation parameter shown in equation (21), a lower p_{FK} should be chosen on practical basis, in the interest of enhancing the projectile stability during the roll speed keeping period.

Table 1
Physical properties for 155 mm dual-spin projectile.

Parameter	Value	Parameter	Value
m_A/kg	41.316	d/m	0.155
m_F/kg	1.482	S/m^2	0.01887
$I_x^A/(kg\cdot m^2)$	0.133	c_V	0.002
$I_x^F/(kg\cdot m^2)$	0.014	c_R	4×10^{-5}
l_{CG}/m	0.6	$g/(m\cdot s^{-2})$	9.8

Table 2
Aerodynamic coefficients for 155 mm dual-spin projectile.

Mach	0.9	0.95	1.1	1.5	2.0
C_D^F	0.082	0.108	0.139	0.074	0.056
C_D^A	0.176	0.221	0.302	0.283	0.230
$C_{L\alpha}$	1.106	1.006	1.273	2.414	2.634
$C_{M\alpha}$	6.667	6.829	7.909	3.941	3.775
C_{Mq}	−24.182	−27.196	−26.243	−15.978	−13.312
C_{rd}^F	−0.282	−0.310	−0.284	−0.112	−0.075
C_{rd}^A	0.004	0.004	0.004	0.002	0.002
$C_{yp\alpha}^A$	−0.450	−0.800	−0.710	−0.610	−0.550
$C_{yp\alpha}^F$	−0.800	−1.400	−1.250	−1.080	−0.960
$C_{Mp\alpha}^A$	0.400	0.560	0.480	0.430	0.380
$C_{Mp\alpha}^F$	0.500	0.700	0.610	0.540	0.480
$C_{N\delta}$	0.172	0.195	0.170	0.076	0.092
C_{rc}	−0.022	−0.025	−0.022	−0.010	−0.006

3.2.3. Roll angle switching period

At the starting and ending point of the roll angle switching period, the variation of rotation speeds of the forward body during this period Δp_{FAS} is a specific value. As γ_F at the beginning and ending of roll angle switching period (recorded as γ_{FASB} and γ_{FASE} respectively) are commanded by the guidance system, considering the operational principle of the actuator of the dual-spin projectile with fixed canards, the variation of γ_F during this period should satisfy the equation $\Delta\gamma_{FAS} = \gamma_{FASE} - \gamma_{FASB} + 2K\pi$, where K can be any integer.

Similarly to the analytical method used in the roll speed controlling period, ΔM_{mo} is decomposed into the average value ΔM_{moa} and the vibration ΔM_{mov}, so that Δp_{FAS} and $\Delta\gamma_{FAS}$ can be expressed as

$$\begin{cases} \Delta p_{FAS} = I_x^{F(-1)} \Delta M_{moa} t_s \\ \Delta\gamma_{FAS} = I_x^{F(-1)} I_2(\Delta M_{mov})\Big|_{t_b}^{t_e} \end{cases} \tag{35}$$

where t_s means the control time of the roll angle switching period. For the sake of the requirements of guidance system, the control time of this period is quite short compared to that of roll angle keeping period followed with it. As is analyzed above, the stability is independent on the control strategy during the roll angle keeping period, so that the stability at the ending point should be studied instead of that during the roll angle switching period.

Substituting equation (35) into equation (27), the stability at the ending point of this period can be expressed as

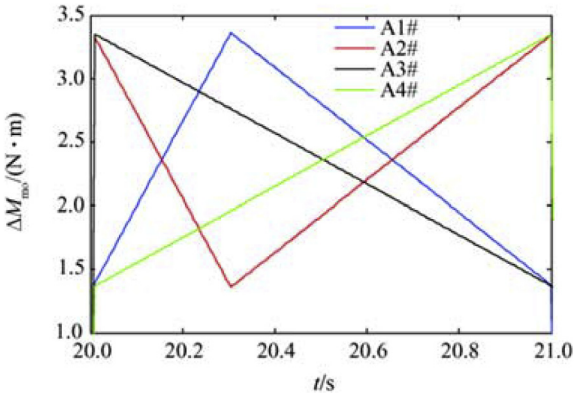

Fig. 6. ΔM_{mo} of different control strategies ($t_v = 1$s).

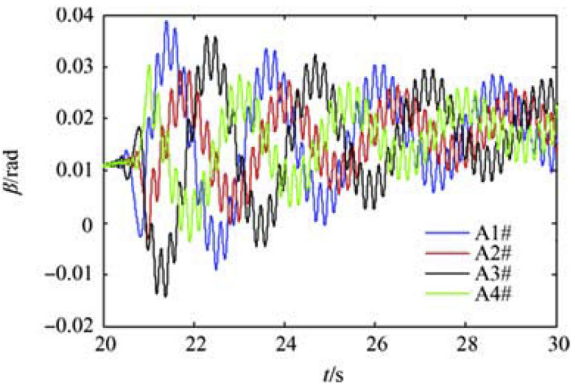

Fig. 7. Angle of sideslip versus time under different$\Delta M_{mo}(t_v = 1s)$.

Table 3
S_p and convergence rate with different$\Delta M_{mo}(t_v = 1s)$.

ΔM_{mo}	A1#	A2#	A3#	A4#
$S_p(10^{-3})$	10.7	6.1	10.6	6.2
Convergence rate/(rad·s-1)	0.0060	0.0034	0.0055	0.0036

$$G_{t_e} = I_{xF}(K_3\Delta p_{FAS} + K_4\Delta\gamma_{FAS}) \tag{36}$$

From equation (36), several results can be obtained that.

(1) The stability of projectile is irrelevant to the control strategy of ΔM_{mo} during the roll angle switching period when $\Delta\gamma_{FAS}$ is definite;
(2) when $K_4 > 0$, the larger K is, the more stable the projectile is; when $K_4 < 0$, on the contrary.

4. Simulations

To verify the influence of control strategies on the flight stability deduced above, nonlinear trajectory simulations are run for 155 mm dual-spin projectile with fixed canards. All simulations results are obtained from a fixed-step (0.005s), forth-order Runge-Kutta numerical integration of the 7DOF equations of motion. The shells are launched from 0 m under the initial conditions of $V = 630\text{m}\cdot\text{s}^{-1}$, $\theta = 45°$ and $p_A = 1277\text{rad}\cdot\text{s}^{-1}$. The physical properties and the aerodynamic coefficients for the 155 mm dual-spin projectile are listed in Table 1 and Table 2 respectively.

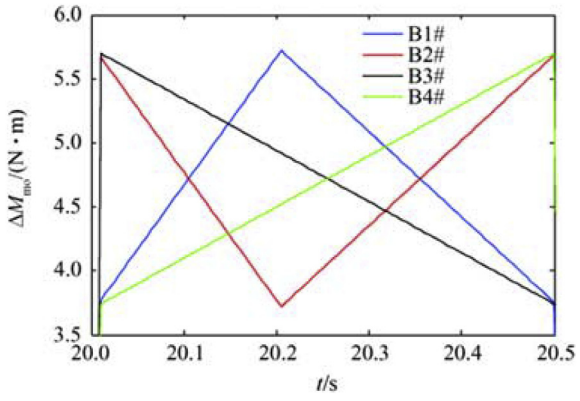

Fig. 8. $\Delta M_{mo}$of different control strategies($t_v = 0.5$s).

Table 4
$S_p$and convergence rate with different$\Delta M_{mo}(t_v = 0.5s)$.

ΔM_{mo}	B1#	B2#	B3#	B4#
$S_p(10^{-3})$	6.6	5.3	7.3	4.7
Convergence rate/(rad·s-1)	0.0030	0.0026	0.0031	0.0024

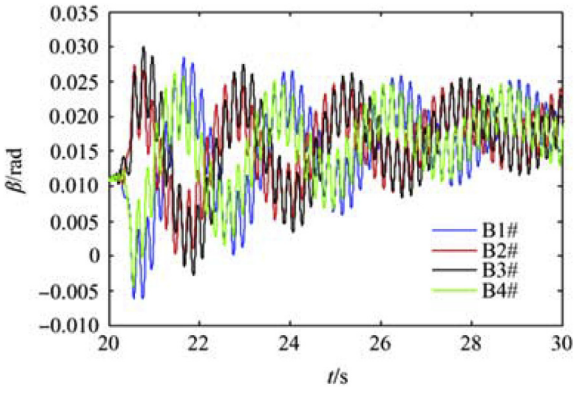

Fig. 9. Angle of sideslip versus time under different$\Delta M_{mo}(t_v = 0.5s)$.

4.1. Roll speed controlling period

In these 7DOF simulations, the roll speed controlling period which starts at 20s, under different control strategies is followed with the same free ballistic flight. In order to avoid the influence of the subsequent control state, p_F after the roll speed controlling period is kept as 5 rounds per second ($r \cdot s^{-1}$). The parameters K_3, K_4 at 20s of the trajectory are 0.0311 and −0.0442 respectively, so K_3/K_4 during this period can be estimated as −0.704. According to the theoretical analysis above, when $t_v = 1s$, the motor torque first ascending and then descending taken the turning point as 20.3s is recommend; when $t_v = 0.5s$, the monotone increasing one is.

When control time $t_v = 1s$, in order to investigate the stability of projectile under different motor torques, a set of ΔM_{mo} shown in Fig. 6 are applied at the projectile under the same initial conditions before the roll speed controlling period. The angular motions of the 155 mm projectile during 20–25s under different control strategies are shown in Fig. 7.

As the result of stability comparison under different control strategies during this period is variable, it is unjustified to compare the angular motion at any time of this period. Considering the subsequent roll speed keeping periods of these trajectories are at the same p_F ($5r \cdot s^{-1}$), whose influence to stability is the same, it is

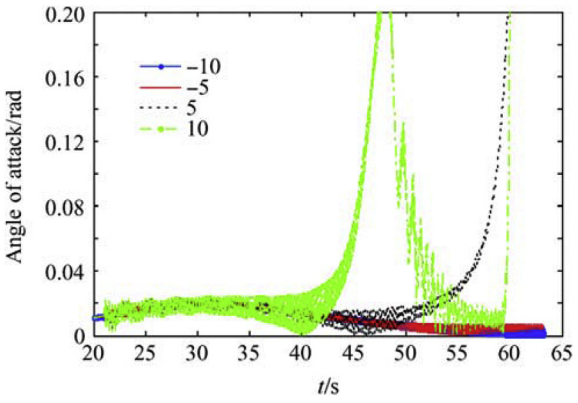

Fig. 10. Angle of attack under different roll speed of the forward body.

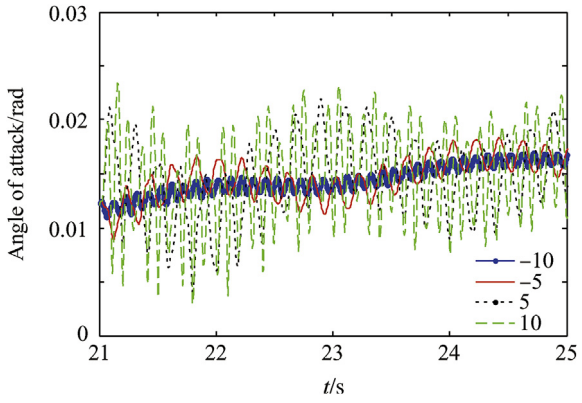

Fig. 11. Zoom view of angle of attack under different roll speed of the forward body.

reasonable to compare the stability under different control strategies of the roll speed controlling period based on the convergence rate of angular motion during the roll speed keeping period. The theoretical approximate calculated values of S_p with different ΔM_{mo} (shown in Fig. 6) and the average of convergence rate of α and β during the roll speed keeping period obtained by simulations are shown in Table 3.

Table 3 and Fig. 6 shows that the trajectory corresponding to the larger theoretical stability assessment characteristic S_p has larger convergence rate during the roll speed keeping period, and the largest S_p and convergence rate are obtained under A1# ΔM_{mo} which is increasing before 20.3s and decreasing after that.

Similarly to the simulations above, when the control time of roll speed controlling period is set as 0.5s, the angular motions of the 155 mm projectile during 20–25s under different control strategies in Fig. 8 are shown in Fig. 7, and the corresponding S_p and convergence rate of angular motion are listed in Table 4.

Figs. 8 and 9 and Table 4 demonstrate that the change trend of the convergence rate and S_p under different ΔM_{mo} are the same, and the largest one is obtained under B3#, which is monotonously decreasing.

To conclude, these simulation results of different t_v (0.5s or 1s) are in line with the theoretical analysis.

4.2. Roll speed keeping period

To verify the theoretical analysis results of the roll speed keeping period, 7DOF simulations are run under the same initial conditions with different roll speed of the forward body ($-10r \cdot s^{-1}$,

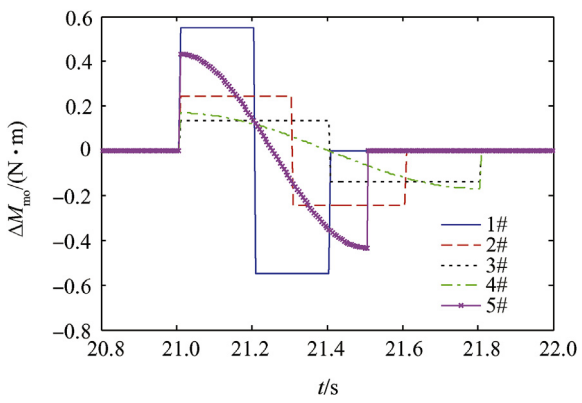

Fig. 12. ΔM_{mo} of different control strategies in roll angle switching period.

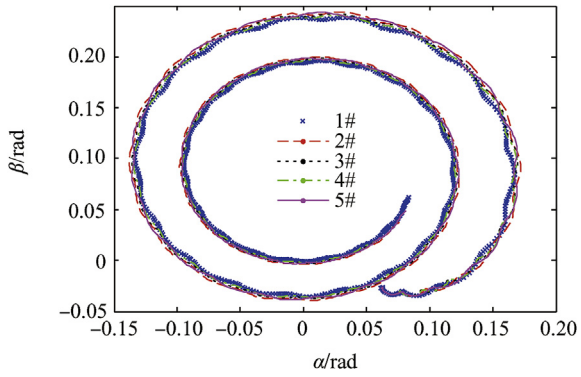

Fig. 13. Angular motion under different ΔM_{mo}during roll angle switching period.

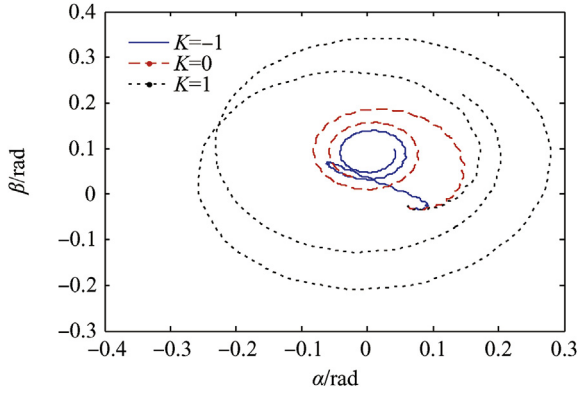

Fig. 14. Angular motion under different$K$ during roll angle switching period.

-5r·s^{-1}, 5r·s^{-1} and 10r·s^{-1}). In order to avoid interfering by the other control periods, only the roll speed keeping period is taken place in these simulations.

The angle of attack of these simulations and the zoom view of it are shown in Fig. 10 and Fig. 11 respectively. Fig. 10 shows that the angle of attack shots up at 40s when $p_F = 10r\cdot s^{-1}$; shots up at 45s when $p_F = 5r\cdot s^{-1}$; changes smoothly when $p_F = -5r\cdot s^{-1}$ or $-10r\cdot s^{-1}$. In other words, the whole trajectory is stable when $p_F = -5r\cdot s^{-1}$ or $-10r\cdot s^{-1}$; unstable at 45s when $p_F = 5r\cdot s^{-1}$ and at 40s when $p_F = 10r\cdot s^{-1}$. It is observed from Fig. 11 that greater p_F is relatively to larger magnitude of angle of attack during this period under the same initial conditions. These simulation results show that the flight stability decreases with the increasing of p_F, which is consistent with the theoretical results.

4.3. Roll angle switching period

The simulations of the influence of control strategy during roll angle switching period on stability of the projectile are divided into two parts: the same $\Delta\gamma_F$ and different $\Delta\gamma_F$.

In the simulations of the same $\Delta\gamma_F$, the roll angle switching period begins at 21s, and the γ_F is switching from 180° to 270°. The initial conditions and control strategies during the flights other than the roll angle switching period are the same. The angular motions of the projectile during 21–25s under different control strategies (shown in Fig. 12) are shown in Fig. 13.

Figs. 12 to 13 demonstrate that p_A after the roll angle switching period under different control strategies are nearly the same; the angular motions under different control strategies are similar numerically. These phenomena conform to the stability analysis during the roll angle switching period when $\Delta\gamma_F$ is the same.

Simulations are running with $\Delta\gamma_F = 0.5\pi + 2K\pi(K = 0, \pm1)$ and the same control time of this period 1.5s. The initial conditions and parameters of these simulations are the same with the previous simulations. The angular motion with different K value during 21–25s is shown in Fig. 14.

Fig. 14 demonstrates that the angle of attack is increasing with K, especially the angular motion goes unstable when $K = 1$. In sum, to satisfy the same command from guidance system, the projectile's stability descends with the increasing $\Delta\gamma_F$. Since K_4 at this time is approximately equal to −0.046 which is negative, the phenomena in the aforementioned simulations conform to the theoretical predictions very well.

5. Conclusion

The influence of control strategy is investigated on the stability of the dual-spin projectile with fixed canards in this effort. Using the projectile linear theory and the Hurwitz stability criterion, the linearized angular motion and the stability criterions have been formulated. To study the influence of the control strategy on stability, a parameter for assessing the impact is defined through comprehensive consideration of the stability criterions. For the sake of the difference between the control features, the controlling flight is separated into three periods, and the influence of control strategy is studied in these parts separately.

Based on the theoretical analysis, the following conclusions can be obtained. To evade or decrease instability risk of the projectile with fixed canards.

(1) A pair of spin canards whose roll moment is as small as possible should be designed;
(2) A lower p_{FK} should be chosen on practical basis during the roll speed keeping period;
(3) During the roll speed controlling period: ΔM_{mo} should increase when $K_3 - K_4(t - t_b - t_v) < 0$ and decrease when $K_3 - K_4(t - t_b - t_v) > 0$;
(4) During the roll angle switching period: when is definite, the stability of projectile is irrelevant to the control strategy of ΔM_{mo} during the roll angle switching period; when $K_4 > 0$, the larger $\Delta\gamma_{FAS}$ is, the more stable the projectile is, vice versa.

Numerical simulations of 155 mm dual-spin projectiles indicate that the influence of control strategies on the stability gives satisfactory agreement with numerical results.

References

[1] Moorhead S. Precision guidance kits (PGKs) improving the accuracy of conventional cannon rounds. Field Artill 2007:31–3. Jan.-Feb.
[2] Grignon C, Cayzac R, Heddadj S. Improvement of artillery projectile accuracy. In: Proc., 23rd international symposium on ballistics. Tarragona, Spain: International Ballistics Committee; 2007. p. 747–54.
[3] Knudson A, Moratz M, Altamura F. The future of fun-fired precision munitions (GFPM). Army AL T 2008:22–5. Jan.-March.
[4] Montalvo C, Costello M. Effect of canard stall on projectile roll and pitch damping. Proc. IME G J. Aero. Eng. 2011;225(No.9):703–16.
[5] Cooper G, Fresconi F, Costello M. Flight stability of an asymmetric projectile with activation canards. J Spacecraft Rockets 2012;49(No.1):130–5.
[6] Rogers J, Costello M. Course correction fuze concept analysis for in-service 155mm spin-stabilized gunnery projectiles. In: AIAA guidance, navigation and control conference and exhibit, Honolulu, Hawaii, USA; 2008. p. 18–21.
[7] Costello M, Peterson A. Linear theory of a dual-spin projectile in atmospheric flight. J Guid Contr Dynam 2000;23(No.5):789–97.
[8] Wernert P. Stability analysis for canard guided dual-spin stabilized projectiles. In: AIAA atmospheric flight mechanics conference and exhibit, Chicago, USA; 2009. p. 10–3.
[9] Dalin Z, Shengjing T, Jie G, Rui C. Flight stability of a dual-spin projectile with canards. J Aero Eng 2014;0(No.0):1–14.

[10] Ollerenshaw D, Costello M. Simplified projectile swerve solution for general control inputs. J Guid Contr Dynam 2008;31(No.5):1259–65.
[11] Fresconi F, Plostins P. Control mechanism strategies for spin-stabilized projectiles. Proc. IME G J. Aero. Eng. 2010;224(No.9):979–91.
[12] Chang Sijiang. Dynamic response to canard control and gravity for a dual-spin projectile. J Spacecraft Rockets 2016;53(No.3):558–66.
[13] Theodoulis S, Fassmann V, Wernert P, et al. Guidance and control design for a class of spin-stabilized fin-controlled projectiles. J Guid Contr Dynam 2013;36(No.2):517–31.
[14] Fresconi Frank. Guidance and control of a projectile with reduced sensor and actuator requirements. J Guid Contr Dynam 2011;34(No.6):1757–66.
[15] John C, Thomas B, William F. Fixed canard 2-D guidance of artillery projectiles. Jan. 2006. US Patent, No.6981672, filed 3.
[16] Je S, Jung H, Park M, Cho T. A study on the aero dynamic characteristics for a spin-stabilized projectile with PGK. In: Proc. 26th international symposium on ballistics, miami, USA; 2011. p. 578–86.
[17] Murphy CH. Angular motion of spinning almost symmetric missiles. J Guid Contr Dynam 1979;2(No.6):504–10.
[18] Murphy CH. Instability of controlled projectiles in ascending or descending flight. J Guid Contr Dynam 1981;4(No.1):66–9.
[19] Wang Y, Cheng J, Yu J, Wang X. Influence of yawing force frequency on angular motion and ballistic characteristics of a dual-spin projectile. Defence Technology 2016;12(No.2):124–8.